Near-Infrared Spectral Monitoring of Pluto's Ices II: Recent Decline of CO and N_2 Ice Absorptions

W.M. Grundy[1,2], C.B. Olkin[2,3], L.A. Young[2,3], and B.J. Holler[2,4].

1. Lowell Observatory, 1400 W. Mars Hill Rd., Flagstaff AZ 86001.
2. Remote observer at the Infrared Telescope Facility, which is operated by the University of Hawaii under Cooperative Agreement #NNX-08AE38A with the National Aeronautics and Space Administration, Science Mission Directorate, Planetary Astronomy Program.
3. Southwest Research Institute, 1050 Walnut St. #300, Boulder CO 80302.
4. Laboratory for Atmospheric and Space Physics, University of Colorado at Boulder, 1234 Innovation Dr., Boulder CO 80303.

Corresponding author: Will Grundy
Mailing address: Lowell Observatory, 1400 W. Mars Hill Rd., Flagstaff AZ 86001
E-mail: W.Grundy@lowell.edu
Voice: 928-233-3231
Fax: 928-774-6296

Running head: Decline of Pluto's CO and N_2 Absorptions
Manuscript pages: 12
Figures: 2
Tables: 1

ABSTRACT

IRTF/SpeX observations of Pluto's near-infrared reflectance spectrum during 2013 show vibrational absorption features of CO and N_2 ices at 1.58 and 2.15 µm, respectively, that are weaker than had been observed during the preceding decade. We suggest that rather than disappearing from the observed hemisphere, these volatile ices are becoming harder to see because of increasing scattering by small CH_4 crystals.

1. Introduction

Near-infrared reflectance spectra of Pluto and Charon obtained on 65 nights at NASA's Infrared Telescope Facility (IRTF) during 2001-2012 were recently presented by Grundy et al. (2013; hereafter Paper 1). The spectra are dominated by vibrational absorptions of methane ice on Pluto's surface (for an overview see Cruikshank et al. 1997 and references therein). A few absorptions are caused by ices of nitrogen and carbon monoxide, both overtones of absorptions at longer wavelengths not easily observable from Earth-based telescopes (Owen et al. 1993; Douté et al. 1999). The absorptions of all three ice species are modulated by Pluto's 6.4 day diurnal rotation, enabling constraints to be placed on the longitudinal distributions of the different ices. Over seasonal timescales, varying patterns of insolation are thought to cause sublimation and redistribution of these volatile ices (e.g., Spencer et al. 1997; Trafton et al. 1998). At Pluto surface temperatures of around ~40 K (e.g., Tryka et al. 1994; Lellouch et al. 2000, 2011) all three ices are mobile, but CO and N_2 ices are much more volatile than CH_4 ice (Fray and Schmitt 2009). CO and N_2 ices are also miscible in one another at all concentrations (Vetter et al. 2007), so it is not surprising that their absorptions were found to share similar longitudinal modulations, being stronger by roughly a factor of two when Pluto's anti-Charon hemisphere is oriented toward the observer. The simplest explanation is that the two ices occur together on Pluto's surface. The longitudinal modulations of Pluto's numerous CH_4 ice absorptions have lower amplitude and their maximum absorption is associated with the leading hemisphere[1]. This observation suggests that Pluto's CH_4 ice has a regional distribution quite distinct from that of more volatile CO and N_2 ices, although other scenarios involving regionally varying ice textures or stratigraphic structures could produce comparable longitudinal variability.

Comparing data averaged over 2001-2006 and over 2007-2012, Paper 1 reported that Pluto's CO and N_2 absorptions appeared to be declining over time, although the observed change

---

[1] Pluto's leading hemisphere is the hemisphere centered on 270°E in right-handed coordinate systems where 0° longitude is defined by the direction toward Charon and the Sun rises in the east. The barycenter of the system is near Pluto, so the leading apex is not actually in the center of this hemisphere, but at a longitude of ~300°E.

between those two intervals was only marginally significant for the CO absorption band. Two possible interpretations were considered, one involving a static distribution of ices seen from a gradually changing vantage as Pluto moves along its orbit and one involving changing spatial distributions of ices as a result of seasonal volatile transport. The static, geometric interpretation places the source of CO and N_2 absorptions at lower latitudes that are contributing progressively less to Pluto's disk-averaged spectrum as the sub-Earth latitude moves away from the equator (equinox occurred during the 1980s and by 2012 the sub-Solar latitude had reached 48°N, with north being defined by the direction of the system angular momentum vector). The volatile transport explanation involves CO and N_2 ices sublimating away from the sunlit northern hemisphere. Both factors could be contributing to the observed decline and thus could be difficult to distinguish. One possible way to disentangle the two effects exploits the parallax from Earth's motion around the Sun. Pluto's obliquity is high, so its slow northward progression of the sub-Earth latitude is modulated by the Earth's annual motion, making it possible to schedule a pair of observations during two successive Pluto apparitions such that the sub-Earth latitude and longitude are nearly identical on both dates. Three such geometrically-matched pairs of observations were considered in Paper 1, with little change being observed between the spectrum pairs. This observation was interpreted as favoring the geometric explanation, although the measurement uncertainties were such that a substantial contribution from volatile transport could not be ruled out.

Unlike the CO and N_2 absorptions, Pluto's stronger CH_4 ice absorptions have been gradually increasing in depth, a trend that has endured for some time (e.g., Grundy and Fink 1996; Grundy and Buie 2001), although it may have slowed in recent years, according to Paper I. The change has been more dramatic at some longitudes than others. Again, a geometric explanation was mooted in which CH_4 absorption is especially strong in northern high-latitude regions that are increasingly dominating the disk-integrated spectrum. But the geometrically-matched pairs showed declining CH_4 band strength, contrary to expectation for the geometric explanation, unless it was coupled with simultaneous sublimation loss of CH_4 from the northern hemisphere or reduction in mean optical path length in CH_4 ice due to evolving ice texture.

2. Observations

Continuing our long-term monitoring campaign, we observed Pluto and Charon on seven nights during 2013 using the SpeX infrared spectrometer at IRTF (Rayner et al. 1998, 2003). Procedures for data acquisition and reduction were described in Paper 1 and interested readers are referred there for additional details. We used a 0.3 arcsec slit with SpeX's short cross dispersed mode, resulting in wavelength coverage from 0.8 to 2.4 µm with a typical spectral resolu-

tion in nightly average spectra of around $\lambda/\Delta\lambda \approx 1600$ where λ is wavelength and $\Delta\lambda$ is the apparent full width at half maximum of an unresolved line. Bracketing observations of nearby solar analog star HD 170379 were used to remove instrumental and telluric effects from the spectra, after correcting the star spectra for a slightly hotter than solar effective temperature of ~6500 K. The Pluto spectra are contaminated with variable and undetermined contributions from Pluto's largest satellite, Charon, depending on the nightly location of Charon relative to Pluto as well as the seeing conditions. Observing circumstances appear in Table 1.

Typesetter: Please place Table 1 somewhere near here.

3. Evolving N_2 and CO Ice Absorptions

As in Paper 1, for each night's Pluto reflectance spectrum we computed equivalent widths for the CO and N_2 ice absorption bands by integrating one minus the ratio of the spectrum divided by a continuum function. For the 1.58 µm overtone band of CO ice, we integrated over wavelengths from 1.575 to 1.581 µm, with a linear continuum function being fitted to the data between 1.571 and 1.575 µm and between 1.581 and 1.585 µm. For the 2.15 µm N_2 band, we used wavelengths from 2.130 to 2.165 µm for the band, and 2.115 to 2.130 µm and 2.165 to 2.180 µm for the linear continuum model. Figure 1 compares the new CO and N_2 equivalent widths with the previously published measurements from Paper 1. It is immediately apparent that all seven of the 2013 observations show CO absorptions well below the average behavior seen in the earlier data, indicating a striking decline in absorption by Pluto's CO ice since the earlier observations. The N_2 equivalent widths in the lower panel were also lower on average than before, but less obviously so, owing to greater scatter among the measurements for that band. We caution that the 2.15 µm N_2 band occurs on the shoulder of a much stronger CH_4 ice absorption, the variation of which could contaminate the apparent N_2 equivalent width. The new 2013 data show no comparably striking change in the CH_4 ice absorption bands.

Typesetter: Please place Figure 1 somewhere near here.

The reduction in volatile CO and N_2 ice absorptions is clearly visible in the 2013 data in Fig. 1, but we wanted to explore the time history of these declining absorptions in greater detail. To do this, we took the sinusoidal fit to the entire data set for each ice absorption band as a function of sub-Earth longitude (the dotted curves in Fig. 1) and refit the constant terms to minimize χ^2 separately to data from each year for which two or more observations were available. The resulting year-by-year evolution of this constant term for both ices is shown in Fig. 2. The average CO and N_2 equivalent widths are lower in 2013 than in any previous year, although 2010 is also a

relatively low year. Indeed, it looks as if the decline in N_2 ice absorption could have begun as early as 2007 to 2009. By averaging together data from 2007-2012, Paper 1 had blended three years when Pluto still showed relatively strong CO absorption with three having diminished absorption, diluting the signal of declining CO ice absorption. We are not convinced that apparent individual variations in Fig. 2 from one year to the next are necessarily real, since the temporal sampling was essentially random from year to year, and in some years it was relatively sparse (see Table 1 of Paper 1). For instance, we obtained no observations during 2010 at sub-Earth longitudes near 0°. Also, the sinusoids we fitted to each year's data are unlikely to be the true functional form of the longitudinal variations of Pluto's CO and N_2 ice absorptions. Nevertheless, a picture emerges of declines in Pluto's volatile CO and N_2 ice absorptions that seem to be accelerating in recent years, and possibly even appreciable variations from year to year.

Typesetter: Please place Figure 2 somewhere near here.

We explored the temporal patterns of spectral changes that could be caused by static ice distributions couple with the seasonal geometric evolution by generating Pluto models having various simple distributions of an optically active ice and sampled them as they would be seen from an Earth-based observer during the years spanned by our IRTF observations. The temporal evolution of a few examples are shown in broken, gray broken curves in Fig. 2. In one of these models, the ice was confined to Pluto's southern hemisphere. Another was similar, but with the ice extending up to 20°N latitude. In a third, the ice occurred in an equatorial belt from 20°S to 20°N latitude. Although these sorts of models can match the recent rate of decline, or the average decline over the past 13 years, none of them was able to replicate a relatively steady-state period during 2001-2006 followed by an accelerating decline of CO and N_2 ice absorptions in subsequent years. Since geometric factors cannot match that acceleration (and certainly cannot match year-to-year fluctuations), the observed time history seems to favor the volatile transport scenario, contrary to our earlier conclusion from the geometrically-matched pairs in Paper 1.

Pluto's CH_4 bands can provide a separate indicator of N_2 ice abundance. Close examination of CH_4 bands shows they consist of two components, interpreted as being due to absorption by CH_4 ice itself plus a blue-shifted version of the same band attributed to CH_4 diluted in N_2 ice (e.g., Quirico and Schmitt 1997; Douté et al. 1999). Tegler et al. (2010, 2012) pointed out that two such components can co-exist under conditions of thermodynamic equilibrium if CH_4 exceeds its solubility limit in N_2 (about 5% molar concentration of CH_4 in N_2 ice at 40K) and that the two phases present under such circumstances would be N_2 ice saturated with CH_4 and also CH_4 ice saturated with N_2 at its solubility limit (about 3% N_2 in CH_4 ice at 40K). The solubility

limit compositions are functions of temperature (e.g., Prokhvatilov and Yantsevich 1983; Lunine and Stevenson 1985), but assuming thermodynamic equilibrium at a given temperature, the ratio of N_2 to CH_4 dictates the relative abundances of the two phases. A larger shift indicates more of the CH_4 is in the shifted, CH_4 diluted in N_2 component, and thus there must be a higher N_2 abundance. We used cross-correlation to measure the apparent shifts of the CH_4 bands in our Pluto spectra and found that they were smaller in 2013 than in previous years. The square points in Fig. 2 show how the yearly evolution of the shift of an example band looks similar to the yearly evolution of the N_2 and CO ice equivalent widths, boosting our confidence that the recently accelerating decline in absorption by these volatile ices is real.

4. Discussion

The recent decreases in Pluto's N_2 and CO equivalent widths can be explained more readily by volatile transport removal than by a static distribution coupled with seasonally changing geometry, but both interpretations seem inconsistent with data from stellar occultations during the same time period (Olkin et al. 2013; Bosh et al. 2013). On Pluto, the atmospheric pressure at the surface is supported by vapor-pressure equilibrium over the N_2 ice, and the N_2 ice temperature is equalized over the surface through the atmospheric transport of latent heat (e.g., Spencer et al. 1997; Trafton et al. 1998). Thus, the pressure depends on the absorbed insolation averaged over the N_2 ice. If the observed decrease in the N_2 and CO equivalent widths were due to a decrease in the projected area of those ices as seen from Earth, regardless of whether the decrease was due to changing geometry or to volatile transport, there would be a corresponding decrease in solar illumination of the ice and thus in its net absorption of radiation. Less absorption would in turn lead to a decrease in surface pressure, contrary to the observed rise in the pressure at a reference radius of 1275 km. A concurrent reduction in the albedo or emissivity of the N_2-rich ice could increase net energy absorption, counteracting decreasing sunlit projected area. However, such changes in the surface ices would be inconsistent with a purely geometric solution. They would also have observable consequences for Pluto's brightness at visible and/or thermal wavelengths that have not to our knowledge been reported.

The phase behavior of binary mixtures of N_2 and CH_4 ices mentioned earlier offers an understanding of the observed declines in spectral absorption by Pluto's volatile CO and N_2 ices and in the shifts of the CH_4 bands and also the lack of observed reductions in atmospheric pressure, CH_4 ice absorption, or photometric brightness. Insolation-driven sublimation of N_2 from the N_2-rich phase in the N_2:CH_4 binary system would force a proportional amount of CH_4 out of the N_2-rich phase in order to maintain its composition as dictated by the solubility limit. The exsolved

CH$_4$ would contribute to growth of existing CH$_4$ ice crystals and/or nucleate new ones. The balance between nucleation of new crystals and growth of existing ones would depend on several unknown factors, including their spacing and the diffusion rate of CH$_4$ within N$_2$ ice. But the CH$_4$ crystals seem likely to be small and close-spaced compared with the centimeter or larger spatial scales of scattering within N$_2$ ice estimated from multiple scattering radiative transfer models of Pluto's N$_2$ ice absorption (e.g., Douté et al. 1999; this size is often described as a "grain size", although it could equally be envisioned as a characteristic spacing between scatterers such as voids or fractures in a more compacted material). The growth and/or nucleation of small CH$_4$ crystals in response to sublimation of N$_2$ could reduce the mean free path of photons in the N$_2$ ice, causing the observed N$_2$ absorptions to decrease without reducing the geographic extent of sunlit N$_2$ needed to support the atmosphere. The CH$_4$ bands would appear less shifted because the fraction of CH$_4$ in the CH$_4$-rich phase had increased. Detailed models are still needed to determine if this qualitative picture works quantitatively. That work is in progress, using new laboratory optical constants of the two ice phases, each with the other species at its solubility limit (Protopapa et al. 2013).

NASA's New Horizons probe will fly through the Pluto system in 2015, sending back a wealth of data from its sophisticated suite of instruments (e.g., Young et al. 2008). However, the spectra presented in this paper show Pluto's surface to be evolving on time scales that are short compared with Pluto's 2.5 century heliocentric orbit, but long compared with the duration of the New Horizons flyby. It is crucial to continue regular monitoring of Pluto from Earth-based observatories to help fit the detailed snapshot from New Horizons into the longer term seasonal evolution of Pluto's volatile ices and atmosphere. A combination of observing techniques including near-infrared spectroscopy, visible photometry, frequent stellar occulations, and thermal infrared radiometry can provide powerful constraints on Pluto's seasonal evolution.

Acknowledgments

REFERENCES

Bosh, A.S., et al. (37 co-authors) 2013. The state of Pluto's atmosphere in 2012-2013. American Astronomical Society Division for Planetary Sciences meeting #45 abstract #404.01.

Buie, M.W., D.J. Tholen, and W.M. Grundy 2012. The orbit of Charon is circular. *Astron. J.* **144,** 15.1-19.

Cruikshank, D.P., T.L. Roush, J.M. Moore, M.V. Sykes, T.C. Owen, M.J. Bartholomew, R.H. Brown, and K.A. Tryka 1997. The surfaces of Pluto and Charon. In: S.A. Stern, D.J. Tholen (Eds.), *Pluto and Charon*, University of Arizona Press, Tucson, 221-267.

Douté, S., B. Schmitt, E. Quirico, T.C. Owen, D.P. Cruikshank, C. de Bergh, T.R. Geballe, and T.L. Roush 1999. Evidence for methane segregation at the surface of Pluto. *Icarus* **142,** 421-444.

Fray, N., and B. Schmitt 2009. Sublimation of ices of astrophysical interest: A bibliographic review. *Planet. Space Sci.* **57,** 2053-2080.

Grundy, W.M., and U. Fink 1996. Synoptic CCD spectrophotometry of Pluto over the past 15 years. *Icarus* **124,** 329-343.

Grundy, W.M., and M.W. Buie 2001. Distribution and evolution of CH_4, N_2, and CO ices on Pluto's surface: 1995 to 1998. *Icarus* **153,** 248-263.

Grundy, W.M., B. Schmitt, and E. Quirico 2002. The temperature-dependent spectrum of methane ice I between 0.7 and 5 µm and opportunities for near-infrared remote thermometry. *Icarus* **155,** 486-496.

Grundy, W.M., C.B. Olkin, L.A. Young, M.W. Buie, and E.F. Young 2013. Near-infrared spectral monitoring of Pluto's ices: Spatial distribution and secular evolution. *Icarus* **223,** 710-721.

Lellouch, E., R. Laureijs, B. Schmitt, E. Quirico, C. de Bergh, J. Crovisier, and A. Coustenis 2000. Pluto's non-isothermal surface. *Icarus* **147,** 220-250.

Lellouch, E., J. Stansberry, J. Emery, W. Grundy, and D.P. Cruikshank 2011. Thermal properties of Pluto's and Charon's surfaces from Spitzer observations. *Icarus* **214,** 701-716.

Lunine, J.I., and D.J. Stevenson 1985. Physical state of volatiles on the surface of Triton. *Nature* **317,** 238-240.

Olkin, C.B., et al. (23 co-authors) 2013. Pluto's atmosphere does not collapse. *Icarus* (submitted, preprint available at http://arxiv.org/abs/1309.0841).

Owen, T.C., T.L. Roush, D.P. Cruikshank, J.L. Elliot, L.A. Young, C. de Bergh, B. Schmitt, T.R. Geballe, R.H. Brown, and M.J. Bartholomew 1993. Surface ices and atmospheric composition of Pluto. *Science* **261,** 745-748.

Prokhvatilov, A.I., and L.D. Yantsevich 1983. X-ray investigation of the equilibrium phase diagram of CH_4-N_2 solid mixtures. *Sov. J. Low Temp. Phys.* **9,** 94-98.

Protopapa, S., W. Grundy, S. Tegler, J. Bergonio, H. Boehnhardt, and L. Barrera 2013. Absorption coefficients of the methane-nitrogen binary ice system: Implications for Pluto. American Astronomical Society Division for Planetary Sciences meeting #45 abstract #303.03.

Quirico, E., and B. Schmitt 1997. Near-infrared spectroscopy of simple hydrocarbons and carbon oxides diluted in solid N_2 and as pure ices: Implications for Triton and Pluto. *Icarus* **127,** 354-378.

Rayner, J.T., D.W. Toomey, P.M. Onaka, A.J. Denault, W.E. Stahlberger, D.Y. Watanabe, and S.I. Wang 1998. SpeX: A medium-resolution IR spectrograph for IRTF. *Proc. SPIE* **3354,** 468-479.

Rayner, J.T., D.W. Toomey, P.M. Onaka, A.J. Denault, W.E. Stahlberger, W.D. Vacca, M.C. Cushing, and S. Wang 2003. SpeX: A medium-resolution 0.8-5.5 micron spectrograph and imager for the NASA Infrared Telescope Facility. *Publ. Astron. Soc. Pacific* **115,** 362-382.

Spencer, J.R., J.A. Stansberry, L.M. Trafton, E.F. Young, R.P. Binzel, and S.K. Croft 1997. Volatile transport, seasonal cycles, and atmospheric dynamics on Pluto. In: S.A. Stern, D.J. Tholen (Eds.), *Pluto and Charon*, University of Arizona Press, Tucson, 435-473.

Tegler, S.C., D.M. Cornelison, W.M. Grundy, W. Romanishin, M.R. Abernathy, M.J. Bovyn, J.A. Burt, D.E. Evans, C.K. Maleszewski, Z. Thompson, and F. Vilas 2010. Methane and nitrogen abundances on Pluto and Eris. *Astrophys. J.* **725,** 1296-1305.

Tegler, S.C., W.M. Grundy, C.B. Olkin, L.A. Young, W. Romanishin, D.M. Cornelison, and R. Khodadadkouchaki 2012. Ice mineralogy across and into the surfaces of Pluto, Triton, and Eris. *Astrophys. J.* **751,** 76.1-10.

Trafton, L.M., D.L. Matson, and J.A. Stansberry 1998. Surface/atmosphere interactions and volatile transport (Triton, Pluto, and Io). In: B. Schmitt, C. de Bergh, M. Festou (Eds.), *Solar System Ices*, Kluwer Academic, Dordrecht, 773-812.

Tryka, K.A., R.H. Brown, D.P. Cruikshank, T.C Owen, T.R. Geballe, and C. de Bergh 1994. Temperature of nitrogen ice on Pluto and its implications for flux measurements. *Icarus* **112,** 513-527.

Vetter, M., H.J. Jodl, and A. Brodyanski 2007. From optical spectra to phase diagrams: The binary mixture N_2-CO. *Low Temp. Phys.* **33,** 1052-1060.

Young, L.A., et al. (27 co-authors) 2008. New Horizons: Anticipated scientific investigations at the Pluto system. *Space Sci. Rev.* **140,** 93-127.

Table 1

Observational Circumstances

UT date of observation mean-time	Sky conditions	H band seeing (″)	Sub-Earth longitude[a] (°E)	Sub-Earth latitude[a] (°N)	Phase angle (°)	Pluto integration time (min)
2013/05/21 13^h.90	Clear	0.4	44.9	49.7	1.17	64
2013/06/01 12^h.78	Partly cloudy	1.0	147.7	49.5	0.90	134
2013/06/12 13^h.56	Patchy cirrus	0.8	246.0	49.3	0.59	66
2013/06/26 10^h.63	Clear	0.7	184.1	49.0	0.20	96
2013/06/27 10^h.62	Clear	0.6	127.7	49.0	0.17	104
2013/06/30 10^h.52	Clear	1.0	318.9	48.9	0.11	100
2013/07/27 8^h.51	Clear	0.5	239.9	48.4	0.76	104

Table notes:

[a.] Throughout this paper, geometry on Pluto is defined as in previous publications of this author, using a right-hand-rule coordinate system in which north is defined by the direction of Pluto's spin vector and east is the direction of sunrise. Zero longitude is defined by the sub-Charon point. Longitudes and latitudes tabulated here were computed by assuming Pluto's spin state is tidally locked to the Buie et al. (2012) orbit of Charon.
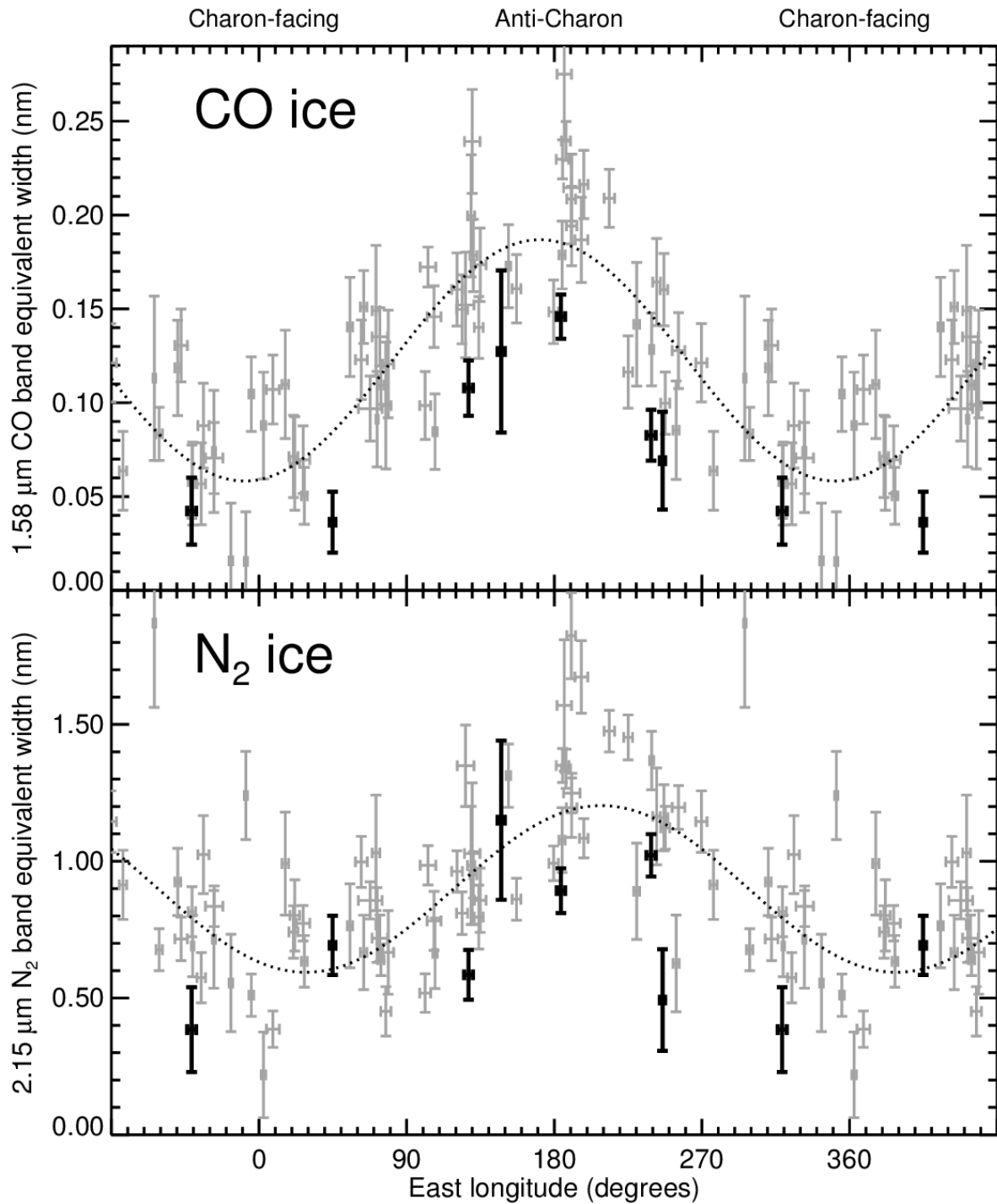
Figure 1. Gray points are the measured equivalent widths of the 1.58 µm CO and 2.15 µm N$_2$ ice bands that were presented in Paper 1 (see Figs. 3 and 6 of that paper). Points are duplicated outside the 0° to 360° longitude interval to better show the periodic character. Black points are for the seven new observations from 2013. Dotted curves are sinusoids fitted to all of the data.
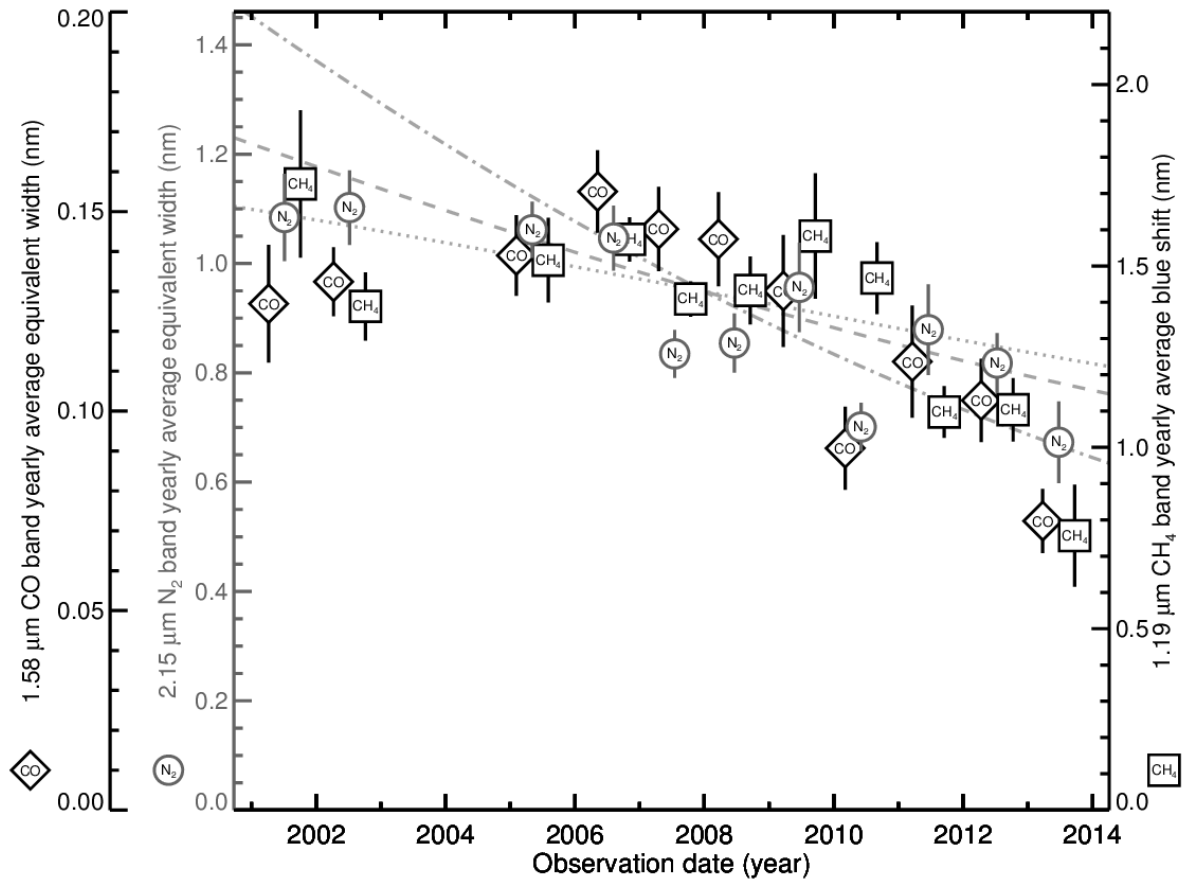
Figure 2. Secular evolution of Pluto's CO and N_2 absorptions as measured by taking the sinusoidal fit to the ensemble data set for each parameter and then refitting just the constant term to each year's data separately. Diamonds (far-left axis) are for the equivalent width of the CO ice absorption at 1.58 µm while gray circles (near-left axis) are for the equivalent width of the N_2 ice absorption at 2.15 µm. Squares are for the blue shift of the 1.19 µm CH_4 band as measured by cross-correlation with a model based on pure CH_4 ice absorption coefficients from Grundy et al. (2002). Diamonds and squares are offset in time by a quarter year to minimize overplotting. The broken-line curves (arbitrarily normalized, and only applicable to the equivalent width data) show secular declines produced by geometric effects with ice-covered regions rotating out of view as the sub-solar latitude moves north. The dot-dash curve is for ice confined to Pluto's southern hemisphere, while the plain dashed curve is for ice on the southern hemisphere plus latitudes up to 20°N. The dotted curve is for an equatorial belt of ice between 20°N and 20°S latitude.